Computer Communications 132 (2018) 74–83

Contents lists available at ScienceDirect

Computer Communications

journal homepage: www.elsevier.com/locate/comcom

WiFO: A hybrid communication network based on integrated free-space optical and WiFi femtocells

Spencer Liverman *, Qiwei Wang, Yu-Jung Chu, Anindita Borah, Songtao Wang, Arun Natarajan, Alan X. Wang, Thinh Nguyen

School of Electrical Engineering and Computer Science, Oregon State University, Corvallis, OR, United States

ARTICLE INFO

Keywords:
Optical communication network
Free-space optical communications
Wireless communications
Hybrid networks
Mobile communications
Electro-optic modulation
Channel characterization
Network protocol

ABSTRACT

Developments in smart home technology and the Internet of Things have significantly increased the demand for high-speed indoor wireless links. Although the majority of the research conducted in this area is still focused on the efficient usage of radio frequency (RF) spectrum, free-space optical (FSO) networks have also been explored as an alternative due to their large bandwidth potentials and low interference. In this paper we present a hybrid FSO and WiFi system (WiFO) that seamlessly integrates optical femtocell architecture with high mobility WiFi networks. Each FSO femtocell in this indoor communication system is capable of transmitting and receiving data at a rate of 50 Mbps over a distance of up to three meters with a field-of-view of ±15°, while still achieving a low bit error rate between 10^{-6}, and 10^{-4}. Reed–Solomon forward error correction codes were also applied to the data stream to further reduce the bit error rate to below 10^{-7}. Different than many other free-space optical communication network using static transceivers, mobility in our WiFO system is achieved through the integration of a WiFi channel in the network protocol. The WiFi channel provides a feedback mechanism and allows for seamless handoffs between FSO femtocells. Additionally, we have experimentally demonstrated the advantage of this WiFO architecture by comparing the throughput of our system with a standard WiFi link in a realistic scenario. Our investigation has shown that the WiFO system presented in this work offers a cost-effective and easy-to-implement approach to significantly increase the capacity of current WiFi networks.

1. Introduction

The number of wirelessly connected devices worldwide is currently experiencing explosive growth. Today there are more than two billion WiFi enabled smart phones and tablets, and that number is expected to increase to more than four billion by 2020. As the number of internet-connected devices continues to climb, so does the demand for data throughputs. Cisco estimates that smart devices worldwide will generate nearly 30 exabytes of data per month by 2020, up from less than 5 exabytes in 2015 [1]. To keep up with this massive increase in demand, wireless networks will have to revolutionize their infrastructure. For more than a decade, WiFi has dominated in wireless networking, and the technology has seen steady improvement during that time period; however, WiFi is intrinsically limited because it uses narrow bands centered around 2.4 GHz and 5 GHz. Recent efforts to increase WiFi data rates have led to highly efficient use of the available 2.4 GHz and 5 GHz radio frequency bands [2–4], but these efforts have not overcome fundamental limitations caused by restricted bandwidths. WiFi access points (APs) are also often shared among several users, which results in a division of the available bandwidth between each user. If the WiFi AP in question is located too close to an adjacent AP, the two signals can interfere with one another causing adjacent and co-channel congestion.

A solution to these problems can be achieved utilizing much higher carrier frequencies in the optical spectrum [5]. Optical frequencies are unregulated and do not interfere with radio signals. Additionally, optical transmissions tend to be line-of-sight (LOS) systems, which offer a physical layer of protection. Any user outside a narrow cone of light would be unable to recover the transmitted message. This LOS property impedes mobility, but also allows multiple access points to be deployed in the same operational space. Each of these access points provides an independent data link to a section of workspace through a free-space optical (FSO) luminary. Reducing the size of the wireless cell to the area of a single light cone increases the bandwidth available to each end user by reducing the number of users accessing any given cell. In a femtocell system, the size of the cell is reduced to the point where only one or two users are accessing a wireless cell at a time [6]. This configuration results in a higher density deployment of wireless cells, but with less mobility within each cell.

* Corresponding author.
E-mail addresses: livermas@oregonstate.edu (S. Liverman), wangqi@oregonstate.edu (Q. Wang), chuy@oregonstate.edu (Y.-J. Chu), boraha@oregonstate.edu (A. Borah), wangso@oregonstate.edu (S. Wang), nataraja@eecs.oregonstate.edu (A. Natarajan), wang@eecs.oregonstate.edu (A.X. Wang), thinq@eecs.oregonstate.edu (T. Nguyen).

https://doi.org/10.1016/j.comcom.2018.10.005

Available online xxxx

In the field of FSO communication, commonly referred to as LiFi, much of the research to date has been focused on outdoor communication links [7,8]. However, most of the problems addressed in that body of research, including long distance attenuation, scintillation, and fading, are not present in WiFO. Although the indoor channel condition for FSO links has not been widely studied, there are several recent proposals and models detailing a joint optimization involving the simultaneous use of both RF and FSO channels [9–14]. While these works are certainly important, they do not demonstrate a well-integrated system incorporating existing WiFi and lack a real world demonstration of the mobility protocol.

Our approach to overcome the inherent issue of mobility in femtocell optical networks is to combine FSO and RF architectures together in a new hybrid system called WiFO. The problem that WiFO seeks to overcome is one that is very common in wireless networks: the seamless handoff from one access point (AP) to another. This problem is very difficult to solve using LOS optics, but can be easily achieved using WiFi signals. Due to the restricted size of a femtocell light cone, it is unlikely that any given user will have to share their FSO connection with many other users. As a user moves out of their light cone and into an adjacent cone, their connection can be seamlessly handed off to the next FSO transmitter in much the same way cellphone connections are handed off from one tower to the next. In this paper we present our current WiFO prototype, which provides up to 50 Mbps of bandwidth per FSO femtocell. This system is capable of streaming data over both FSO and WiFi channels. The versatility of this hybrid architecture provides improved performance and mobility when compared to stand-alone FSO or WiFi systems.

2. Related work

Recently, several efforts have been made to demonstrate the potential of FSO networks utilizing commercially available white light emitting diode (LED) fixtures [15–18]. These fixtures are attractive due to the fact that they can serve as both a visible light communications (VLC) luminary and communications link. However, LED luminaries are often hindered by relatively long response times, limiting their bandwidths. The two main types of LED luminaries currently under research are red/blue/green (RGB) LEDs [19–21] and white phosphor LEDs [22]. RGB LEDs are often capable of higher modulation bandwidths and allow for wavelength division multiplexing (WDM), but produce a spectrum of light that is less pleasing to the eyes. White phosphor LEDs produce a warmer wide spectrum, but their modulation bandwidths are limited by the slow-reacting phosphor coating on the bulb. White phosphor LEDs are currently preferred for commercial and domestic lighting applications and it has been shown that using these luminaries as a transmitting source does not significantly degrade the quality of their output spectra [23]. Techniques such as filtering out the slower reacting phosphor light and pre-equalizing the LED's driving circuit have been used to extend the 3 dB bandwidth of white LEDs from just a few megahertz to nearly 20 MHz; however, this was demonstrated over a distance of just 10 cm [24]. The limited range of this system can be attributed to the relatively low 20% modulation depth of the transmitted optical signal.

In an effort to overcome the relatively low modulation bandwidth of LEDs, spectrally efficient modulation schemes such as QAM, OFDM, and DMT have been explored [25–27]. Although these schemes utilize available bandwidth more efficiently, they also require a significantly higher received SNR. Even a simple four level pulse amplitude modulation (PAM4) scheme would require an additional 6 dB of optical output power [28]. Reducing the solid angle of the transmitting optical source can dramatically increase the power density at a receiver; however, any reduction in solid angle will result in a reduction in mobility. Well-collimated point-to-point FSO systems have also been proposed [29], but point-to-point systems necessitate an accurate indoor positioning system such as time difference of arrival (TDOA) [30] and a beam steering mechanism. These additional components increase complexity and reduce cost effectiveness.

In addition to lighting fixtures, micro-light-emitting diode arrays have also been explored as transmitting sources [31]. These arrays have been shown to have bandwidths well in excess of 100 MHz, but with output powers of less than 1 mW. These devices are entirely unsuitable for free-space applications. In a normal office environment, the distance from the floor to the ceiling is roughly 3 m. If the average desk height is assumed to be 70 cm, any commercial FSO system must have a range of at least 2.3 m. Diffuse FSO optical transmissions of 10 Mbps over a distance of 2.3 m have been demonstrated using white LEDs; however, the question of mobility was not addressed in that work [32].

In visible light FSO networks utilizing LED luminaries, the power of the transmitter is directly linked to the brightness of the bulb. One solution to the brightness problem is to simply decouple the FSO network from the task of illumination by replacing the visible light LEDs with infrared (IR) LEDs [33]. IR LEDs are invisible to the human eye, and can therefore be driven at any brightness level without disturbing network users. Additionally, IR LEDs operating at 850 nm are inexpensive, widely available, and their wavelength corresponds closely to the peak responsively of silicon photodiodes [34].

In regard to hybrid FSO/RF networks, work has been completed characterizing data throughputs, delay, and the effect of distance on high performance outdoors FSO systems [35,36]. For indoor environments, Light-Fidelity (LiFi) has been proposed as a hybrid FSO/RF system. LiFi utilizes LEDs as both transmitters and luminaries [37,38]. One possible advantage of this model is that the power lines themselves could be used as a low speed connection between LED luminaries. This power line communication scheme could then be used to coordinate VLC transmissions between overlapping luminaries [39]. Although the integration of lighting and communications systems might initially seem like a simplification, it would require a massive shift in the manufacturing of lighting components and a complete retrofit of old lighting fixtures. In contrast, the proposed WiFO system utilizes inexpensive IR LEDs that are invisible to the human eye and do not require any integration with existing lighting fixtures [40,41].

From a wireless network design prospective, one of the critical issues that must be addressed is the handoff mechanism between APs. FSO systems can leverage some of the work compiled for RF systems; however, there are several networking challenges that are unique to LOS systems such as the density of deployed APs. One example of this can be found in the multi-armed bandit model, which has been applied to FSO handoff strategies in an attempt to optimize the exploitation vs exploration tradeoff [42]. This model seeks to enhance the gain in a system by balancing the allocation of resources between competing users. In addition, the concept of fuzzy logic systems have been applied to greatly simplify complexity handoff problems [43]. Fuzzy logic systems reduce the complexity of binary decision making by transforming the problem into a list of simple rules that must be followed.

Within a single FSO AP, resource allocation must also be considered. In any FSO network, it is possible that multiple users might try to access the same optical link at the same time. If such an event occurs, it is necessary to have a system is place that can properly allocate resources to each user. To solve this problem, an automatic resource slicing or virtualization scheme has been proposed [44]. This scheme would dynamically create a number of virtual AP within each FSO cell based on the requirements of the system at any given time. The central AP in this scheme analyzes the data traffic from each of the applications supported under it and assigns resources fairly and proportionally between them. The scheduling in this scheme would be based on an extended token bucket fair queuing algorithm, which has already been well established for RF networks. The number of virtual slices that are required for each link can be reduced by reducing the size of the FSO AP.

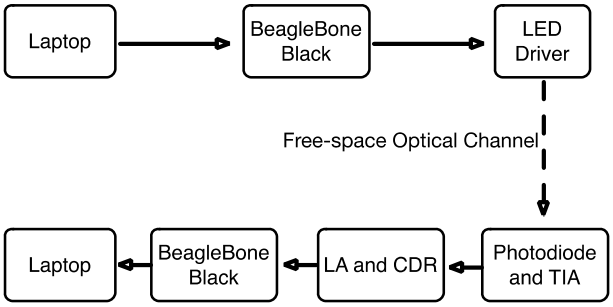

(a)

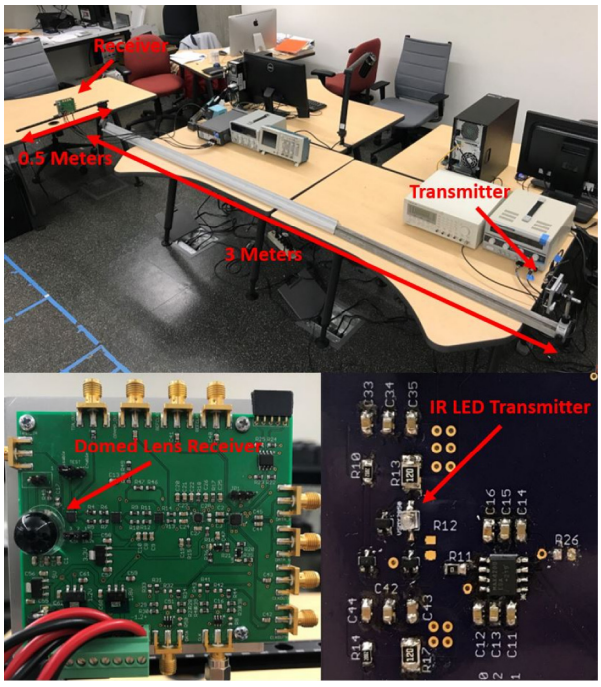

(b)

Fig. 1. WiFO system — (a) high level system block diagram, (b) FSO experimental setup with zoomed views of the optical transmitter and receiver.

3. WiFO system

In this section, we describe the WiFO system that we constructed to demonstrate the potential of our purposed hybrid FSO and RF system. This system consists of a FSO transmitter and a WiFi enabled optical receiver. Both the transmitter and receiver are connected to computers that will serve as APs through a BeagleBone microcontroller. Fig. 1(a) shows a high-level bock diagram of our system depicting the main functional blocks of the system's components as tested. To test this system, we place the FSO transmitter and receiver on a 3-meter-long horizontal optical rail. The receiver was also attached to a perpendicular 0.5-meter rail, which was used for tests involving lateral offsets. Fig. 1(b) shows the FSO experimental set up used for testing.

3.1. Transmitter

The transmitter component includes a BeagleBone Black microcontroller and a LED driver circuit. The BeagleBone microcontroller serves as a conduit between the AP (in this case a laptop computer) and the LED driver. On board the BeagleBone there is a 1 GHz Texas Instrument AM335x CPU, a WiFi antenna, and 200 MHz GPIO pins. These attributes make the BeagleBone an ideal platform for sending a receiving data both through the FSO and WiFi channels. Various functions like modulation and coding on the network, link, and physical layers are handled by the BeagleBone's PRU. After modulation and coding, the BeagleBone passes data to the LED driver in the form of binary serial bits.

The LED driver circuit is shown in Fig. 2(a). The goal of this circuit is to convert an electrical input signal into an optical signal in a simple and cost effective way. The main challenge in developing a robust transmitter design is overcoming the tradeoff between brightness and bandwidth. The LEDs in this design must be capable of transmitting over a distance of at least three meters while being modulated at frequencies in the tens of megahertz. Larger LEDs are typically brighter, but suffer from high terminal capacitance, which limit their bandwidths. In the transmitter circuit presented here, a VSMY2850 850 nm IR LED diode is modulated using a "swept-out" LED driver based on circuits presented in [45]. This LED driver is designed to operate the IR LED using a simple on–off keying (OOK) modulation scheme. When the LED is in the "on" state, Q3 is turned on and resistor R1 limits the current flowing through the LED, thereby controlling its maximum brightness. When the LED is in the "off" state, transistor Q2 is turned off, which in turn makes transistor Q1 high. Q1 then shorts the two terminals of the LED, reducing the optical fall time. This "sweeping out" of the free carriers remaining in the diode improves performance by reducing the series resistance that dominates the RC delay inside the diode when switching from the "on" to "off" states. Unlike traditional LED modulation schemes, this circuit design does not modulate the LED's brightness around a bias point. Instead the LED is driven in this two state system in which the LED is either transmitting at its maximum possible brightness or turned off completely. Utilizing the LED's full dynamic range maximizes the transmitter's SNR and eliminates the need for a bias tee. Low side driver designs that are similar to this design are also common, but often have low bandwidths due to high RC constants in the "off" state.

The improvement made in optical fall time of the transmitting LED is illustrated in Fig. 2(b). The optical fall time without transistors Q1 and Q2 is 24 ns and is plotted in orange, while the improved 4.3 ns optical fall time, plotted as blue, is measured with transistors Q1 and Q2 in place. This 20 ns reduction in the optical fulltime significantly improves the performance of the transmitter and directly translates to an improvement in the transmitter's frequency response. Fig. 2(c) shows the normalized frequency response of the transmitter with transistors Q1 and Q2 in place. The 3 dB bandwidth of this design is 45 MHz, which is more than sufficient for 50 Mbps transmissions using a simple OOK modulation scheme.

The number of optical transmitters that are required to fully cover a working area is directly related to the viewing angle of the transmitting source. The IR LEDs used in the design presented in this paper have a half viewing angle of 10 degrees. If the LEDs are placed 3 meters above the ground, each LED can cover an area of 3.7 square meters; however, in practice the signal will not be strong enough to serve that entire area. This coverage is largely different than that of point-to-point optical communications systems, which require aspheric lenses and well-collimated beams. Collimating the light emitted from the LED source considerably increases the power density within the beam, but also drastically restricts the angle at which the beam can be viewed. This approach is impractical for a commercial system as it greatly increases both the number of transmitters that is required within a given space and the complexity of each transmitter. Alternatively, the plastic lenses that come pre-packaged with the Vishay LEDs are available for less than a dollar each when bought in bulk. In diffuse FSO systems, power density is usually the limiting factor and should be considered carefully. Table 1 lists each of the transmitter's components and their associated values.

3.2. Receiver

The receiver in this system design is responsible for collecting the transmitted optical signal and converting it back into a stream of binary

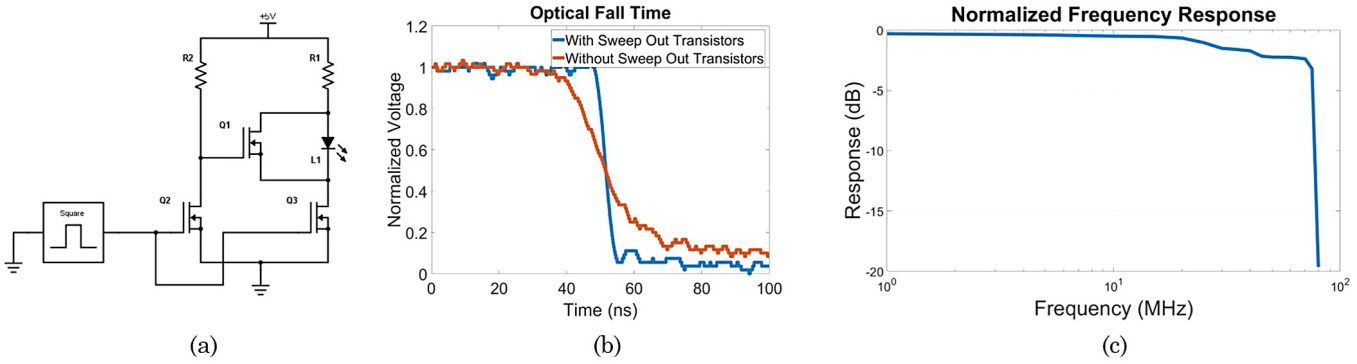

Fig. 2. Free-space optical transmitter — (a) transmitter schematic, (b) improvement of the optical fall time with sweep out transistors included, (c) normalized frequency response.

Table 1
Transmitter components.

Schematic symbol	Description of FSO transmitter components	Part number/ Value
Q1	Shorts L1 when pulled high	AO7404
Q2	Trigger for Q1	AO7404
Q3	LED driver	RSU002N06
L1	LED source	VSMY2850
R1	Current limiting resistor	12 Ohms
R2	Pull up resistor	20 k Ohms

Table 2
Receiver components.

Schematic symbol	Description of FSO receiver components	Part number
PD	Photodiode	S6968-01
TIA	Transimpedance amplifier	OPA857
LA	Limiting amplifier	ADN2890
CDR	Clock-Data recovery circuit	ADN2915
COMP	Comparator	TVL3501

bits. Due to the nature of the OOK modulation scheme used in this design, the task of recovering bits is simply a question of determining whether each bit is a one or a zero. The most straightforward means of accomplishing this task is by saturating the incoming signal and then comparing that signal to some pre-defined threshold. Fig. 3(a) shows a high level diagram of the receiving circuit designed around this principle. First the incoming photons are converted into a photocurrent using a reverse biased PIN diode. That current is then converted into a voltage and amplified by a trans-impedance amplifier. The voltage signal is then saturated by a limiting amplifier and passed to a clock-data recovery (CDR) circuit, which outputs both the recovered bits and the clock signal that was used to generate those bits. Lastly, the recovered bits are sent to a comparator, where their amplitudes and DC levels are adjusted such that they can be directly read back into the Beagle Bone Black microcontroller. The Beagle Bone Black board can then directly interface with a laptop computer or transmit data back to any WiFi connected device.

In an effort to keep the cost of the receiving circuit low, inexpensive PIN diodes were chosen instead of avalanche photodiodes (APDs). APDs are often selected due to their high sensitivities, but these devices are also much more expensive. In our design, we focused on maximizing the brightness of the transmitting source, thereby reducing the need for high sensitivity detectors. Much like the transmitting LEDs, there is a fundamental tradeoff between the size of the PIN diode's active area and its usable bandwidth. As the active area size increases, so does the diode's capacitance. This increase in capacitance then limits the bandwidth of the device by increasing its RC delay. A lens can be used to collect more light into the surface of the diode's active area, but a fundamental tradeoff between the focal length of that lens, the size of the detector, and the angle at which rays can be viewed must be considered. Additionally, there is a more general relationship between the diameter of the lens and the focal length of that lens, wherein larger lenses tend to have longer focal lengths. These two relationships present a significant challenge for collecting light in FSO systems. Ideally, one would like to use a large lens with a particularly short focal length, which would then focus rays at large angles onto a small detector with a low RC delay, but some concession must be made.

With these considerations in mind, a Hamamatsu S6968 PIN diode with a 14 mm plastic domed lens was selected as a receiver. This diode has a 3 dB bandwidth of 50 MHz and an effective area of 150 mm^2. Additionally, the short focal length of the domed lens mounted on its surface allows for relatively large viewing angles. Fig. 3(b) shows a plot of the photocurrent generated by the diode normalized to its maximum value as a function of incident angle. From this plot it is clear that the 3 dB half viewing angle of this diode is 30 degrees. In a real-world working environment, an FSO network user might move positions and change orientations several times. It is critical in such an environment that the optical receiver is capable of operating over a wide range of angles.

To better understand how the optical receiver in this system design will perform in an actual office setting, the receiver's sensitivity was evaluated. The sensitivity of the optical receiver is directly related to the photocurrent generated by the PIN diode. In the FSO receiver circuit, the only two components that are operating in a linear region are the photodiode and the TIA. If the TIA is generating a voltage that is greater than the minimum sensitivity of the limiting amplifier, the limiting amplifier will saturate that signal to its rail voltage. If the TIA produces a voltage below the limiting amplifier's minimum sensitivity, the output will be zero. Essentially, the limiting amplifier makes a binary decision based on the output of the TIA, and then passes either a 1 or 0 to the CDR circuit. Once a binary decision has been made, the amplitude of the data signal moving forward is no longer a concern. For this reason, it is critical to ensure that the TIA produces a voltage that is large enough to be correctly interpreted by the limiting amplifier. Each of the receiver's components and related parts numbers are listed in Table 2.

The Analog Devices limiting amplifier that we have chosen in this receiver design has a minimum sensitivity of 4 mV_{p-p} and the Texas Instruments TIA has a selectable trans-impedance gain of either 4.5 k ohms or 18.2 k ohms. Using these two pieces of information it is easy to calculate that in the worst case the photodiode must generate just under 1 μA of photocurrent to ensure that the limiting amplifier correctly interprets the data signal. Fig. 3(c) plots the photocurrent measured from the output of the photodiode as a function of distance. The photodiode is still producing a current of roughly 7.8 μA at a distance of three meters, more than seven times the amplitude required for the limiting amplifier. When the photodiode is rotated such that the incident light hits the detector at an angle of 30 degrees, the photocurrent is reduced by about 50% to roughly 3.9 μA. While the data signal should still be recoverable at this angle, the receiver is nearing

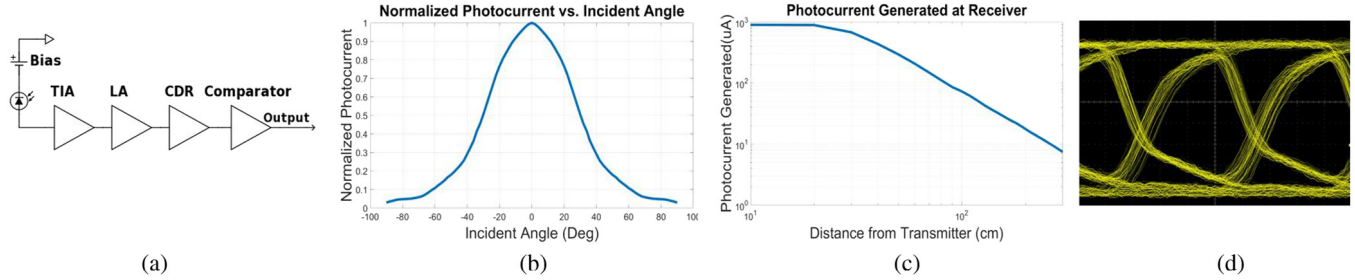

Fig. 3. Free-space optical receiver — (a) receiver block diagram, (b) photodiode angular dependence, (c) photocurrent generated at the receiver, (d) eye diagram showing a 50 Mbps received signal sent over a distance of one meter before the signal is saturated by the limiting amplifier.

its detection limit. Fig. 3(d) shows an eye diagram taken at a distance of 1 meters and at a data rate of 50 Mbps before the signal is saturated by the limiting amplifier.

3.3. Network protocol

A custom network protocol stack was created to ensure that our system hardware functioned correctly. Specifically, the physical, data link, network, and transport layers were defined and an application was created to handle the necessary data flow processes. In this section, we will provide a brief description of each layer and detail essential aspects of application running on the Ethernet connected AP.

3.3.1. Physical layer

On the physical layer, a simple OOK modulation scheme is used to maximize SNR. High intensity light corresponds to a logic high state, while low intensity light corresponds to a logic low state. Manchester coding is also used to ensure the regular bit transitions that are necessary for clock recovery on the receiving end. The CDR on the receiver will sample data on the rising and falling edge of the recovered clock signal. Unlike WiFi transmissions, our FSO transmitter is a LOS device and therefore does not experience multipath fading. Reflections from objects and surfaces within the work environment do not significantly affect the received signal. The majority of the bit errors observed in this system are caused by inter-symbol interference (ISI). This ISI is a direct result of the transmitting LED's limited frequency response.

3.3.2. Data link layer

The data link layer in this stack is very straightforward. Each of the FSO link frames is broken down into a preamble and a payload. The preamble consists of 32 bits and is used to distinguish one frame from another. The payload consists of 612 bytes and contains the data for each frame.

3.3.3. Network layer

The network layer in our system is different from normal network layers in that it handles the mobility protocol in addition to routing packets to their destinations. Our network layer packets consist of 12 bytes of packet header and 600 bytes of data related to the upper layers. Within the packet header 4 bytes are the FSO transmitter ID, 4 bytes are the receiver ID, and 4 bytes are the packet ID. First, transmitter ID is used to determine which transmitter will send the optical signal. Second, the receiver ID is used to determine the packet's destination if multiple receivers are paired with a single optical transmitter. Third, the packet ID is used to determine whether or not packets successfully reached their destinations. If the packets are delivered successfully, an acknowledgment is sent back to the AP. If the AP does not receive an acknowledgment for a packet, the packet ID is used to determine which packet was lost.

The AP continuously records the status of all of the receivers that are active in the work area. The receiver status includes information like IP addresses, packet IDs for packets that they have received, and a transmitter ID for the transmitter that is currently associated with that receiver. When a receiver enters a WiFO network for the first time it connects to the AP through a WiFi channel and then looks for a beacon signal. If a beacon signal is found, the receiver updates its status with the AP. If a beacon signal is not found, a timeout acknowledgment is sent to the AP and the receiver's status is again updated. On the transmitter side, the transmitter sends all of the packets that it has in its queue. When the transmitter is idle, it sends out a periodic beacon signal for receivers to pick up.

3.3.4. Transport layer

In the proposed WiFO architecture, the FSO channel is unidirectional. Therefore, acknowledgment messages are always sent over the WiFi channel. In our system an acknowledgment is sent for every 10 packets that are received successfully. In an effort to simplify the design of our system, the network layer, transport layer, and mobility protocol are realized in the application layer using the pre-encapsulation method. This approach will allow any future network application easy access to the WiFO system. Drivers for the FSO transmitter and receiver are being developed as a Linux kernel module.

3.3.5. Access point application

The network protocol described in this section is implemented predominantly in an application running on a "smart" AP. The AP in this system controls the WiFi and optical transmitters and keeps track of which channels are available to end users. The application running on the Ethernet connected AP can be broken down into three main threads: data process, FSO manager, and user manager. The data process thread handles the transmission of data across both the WiFi and FSO channels. While WiFi packets are supported for both uplink and downlink, the FSO packets are only sent through the downlink. The WiFi uplink in the data process thread also relays information about the status of an end user's connection back to the AP, which is used in the remaining two threads. The FSO manager thread controls which FSO transmitters are active at any given time. If an FSO transmitter is available to an end user, the FSO manager will activate that transmitter and direct downlink packets through the FSO channel. If the end user moves out of range of that FSO transmitter, the FSO manager will deactivate the transmitter in question. The user manager thread keeps an updated list of users on the network and tracks which uplink and downlink channels they are utilizing. When the status of an end user changes, the user manager will update its user table, which will then be referenced by both the data process and FSO manager threads. A diagram detailing the structure of the AP application, user and FSO cone tables is shown in Fig. 4(a) and (b). Fig. 4(c) defines the formats of packets which keep the user and FSO cone tables updated and ensure the data transmissions. The explanations of columns in the packet formats are as following [46] (see Table 3):

- Cone ID: Each transmitter connected to the AP server gets a unique ID assigned by the server.
- IP Address: This stands for the destination(user) IP address of the packet.

Table 3
Cone ids and users' locations.

Cone IDs	User Location	Server Action
Current Cone ID ≥ 0, Previous Cone ID < 0	Moving into a light cone	Register the user to the table
Current Cone ID < 0, Previous Cone ID ≥ 0	Moving out of a light cone	Delete user from the table
Current Cone ID ≥ 0, Previous Cone ID ≥ 0, Current Cone ID = Previous Cone ID	Staying in a light cone	N/A
Current Cone ID ≥ 0, Previous Cone ID ≥ 0, Current Cone ID ≠ Previous Cone ID	Moving from one light to toward another light cone	Update the table
Current Cone ID < 0, Previous Cone ID < 0	Not moving toward or in any light cone	N/A

• Packet ID: Each data packet has a unique packet ID that the AP server can track via the ack packet if the data is received by the receiver successfully.

• Data Length: This column indicates how many bytes there are in the data payload.

• Data payload: The raw data that has not applied any modulation and coding schemes.

• Identifier: A specific number to distinguish beacon packets from the data packets.

Data packets are encapsulated at the AP server, coded and modulated at the transmitter, then sent to the receiver(user). Beacon packets are generated, coded and modulated at the transmitter, and broadcasted out intermittently. Ack packets are sent to the AP server from the receiver while receiving data packets/beacon packet. Upon the information in the received ack packets, the AP server updates its user and FSO cone tables. Below is a table shows the corresponding user locations and server actions according to the current cone IDs and previous cone IDs from the ack packets.

4. System evaluation

In this section we will evaluate the performance of our WiFO system in terms of transmission distance, transmission angle, throughput, bit error rate (BER), and delay. These metrics are all important factors when building a robust communications network. In each test, packets containing pseudo-random data will be transmitted across the FSO channel using a BeagleBone microcontroller as a source.

On the receiving end, the receiving module will convert the optical signal back into electrical bits and then pass the recovered data to a second BeagleBone board. The second BeagleBone will sample the recovered packets and store the data in memory. In some cases, forward error correction (FEC) coding was applied to the transmitted signal in the form of Reed–Solomon codes. All measurements were taken at a data rate of 25 Mbps unless otherwise stated. In our system evaluation we have considered several spatial parameters. These parameters are illustrated in Fig. 5 and include vertical distance from the FSO transmitter, lateral distance between the transmitter and receiver, and the rotation angle between the transmitter and receiver. When a rotation angle is not given, it can be assumed to be 0°. Factors such as FSO channel round trip time and the transition time between the FSO and WiFi channels were also considered. Throughout this evaluation, the goal will be achieve an uncoded BER of less than 10^{-4}, which can be reduced to a BER of less than 10^{-6} when simple Reed–Solomon FEC codes are applied.

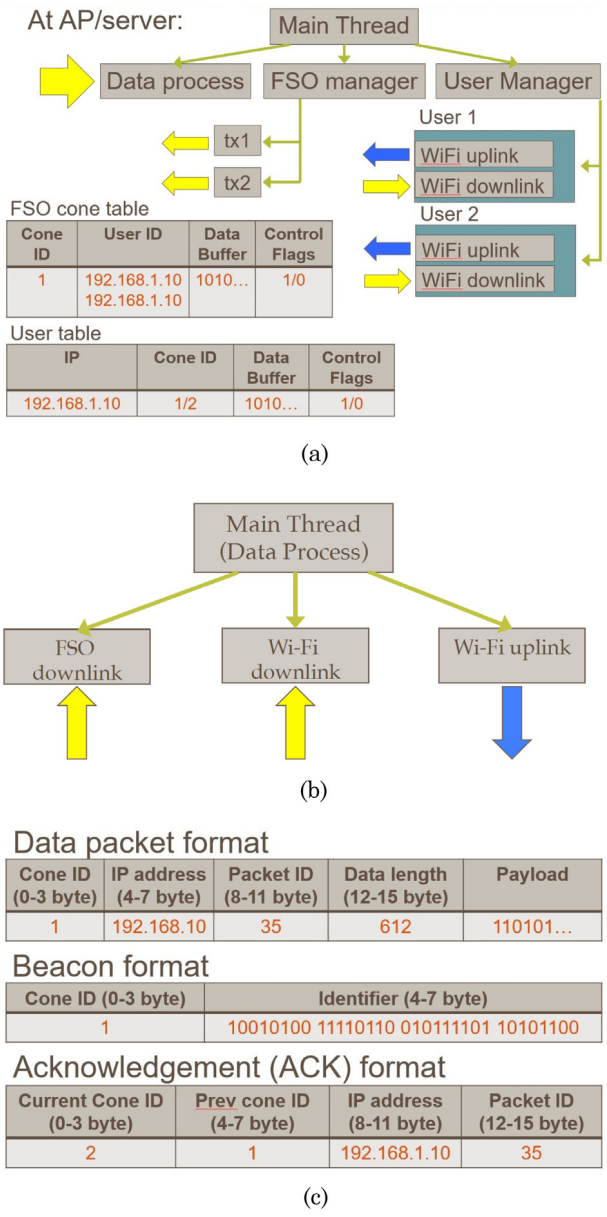

Fig. 4. AP application — (a) application diagram detailing the main threads, user and FSO cone table formats, (b) diagram showing data process sub-threads, (c) formats of packets, which keep the user and FSO cone tables updated.

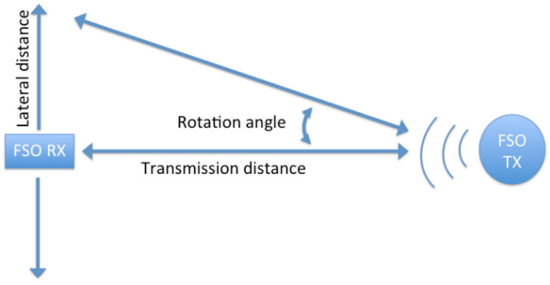

Fig. 5. FSO channel spatial parameters.

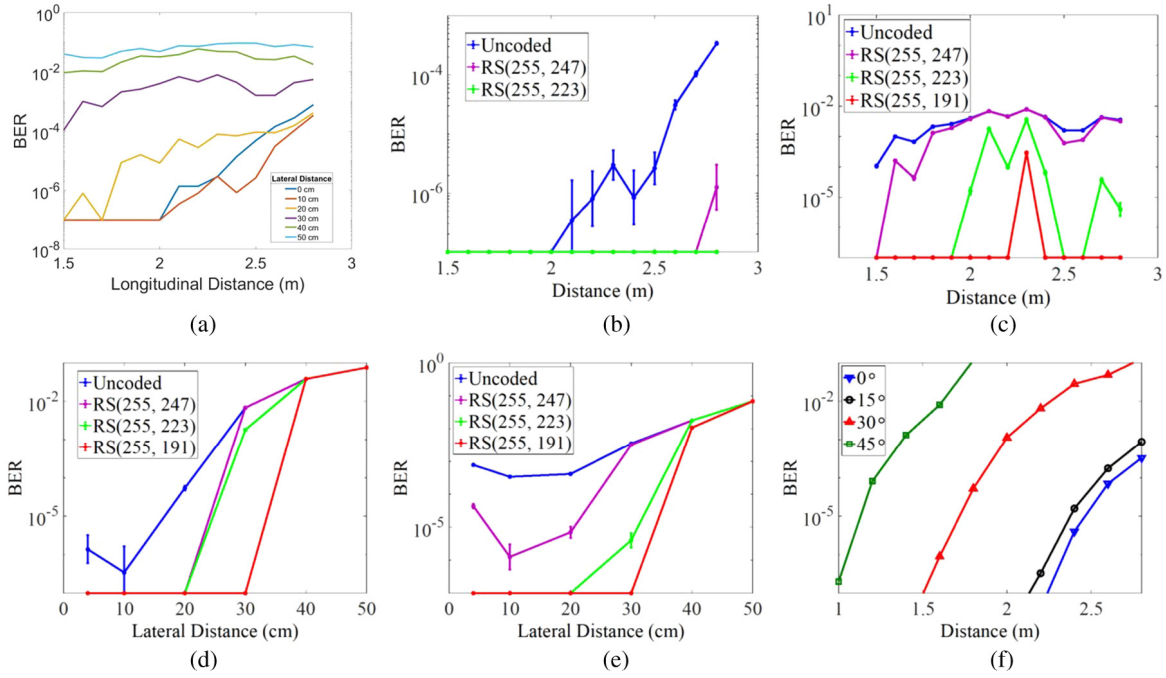

Fig. 6. Bit error rate measurements taken at 25 Mbps — (a) un-coded BER as a function of vertical and lateral distance, (b) Reed–Solomon coded BER with fixed 10 cm lateral offset, (c) Reed–Solomon coded BER with fixed 30 cm lateral offset, (d) Reed–Solomon coded BER with fixed 2.1 m vertical offset, (e) Reed–Solomon coded BER with fixed 2.8 m vertical offset, (f) un-coded BER angular dependence.

4.1. Bit error rate without FEC

An overview evaluation of the FSO channel BER without FEC in terms of vertical and lateral distances is presented in Fig. 6(a). This plot shows the BER of un-coded data for vertical distances between 1.5 and 2.8 m and for lateral distances between 0 and 50 cm. Due to limitations in the BeagleBone hardware, the minimum detectible BER is 10^{-7}. When the lateral distance is less than 20 cm, the BER is below the detection limit for distances less than 2 m. Interestingly, the BER for lateral distances of 0, 10, and 20 cm seem to converge as the vertical distance increases to 2.8 m. This result is most likely due to the fact that the light cone produced by the transmitting LEDs takes on a Gaussian intensity profile. As the cone diverges, points along its lateral profile do not diverge linearly. At points close to the FSO transmitter, the difference between the light intensity in adjacent lateral locations might be very large. As the Gaussian profile expands, those same points would experience a much smaller variation in intensity.

4.2. Bit error rate with FEC — fixed lateral offset

In all commercially available wireless communications systems, FEC is used to drastically improve the BER of transmissions. Fig. 6(b) and Fig. 6(c) show the BER improvements when Reed–Solomon FEC codes are applied to the data. In these figures the vertical distance is varied while the lateral distance is fixed at 10 cm and 30 cm respectively. At a lateral distance of 10 cm, the weaker RS(255,247) and stronger RS(255,223) codes both reduce the BER to well within acceptable levels. In the case of the stronger RS(255,223) code, no errors were detected. When the lateral offset was increased to 30 cm, the BER increased significantly. However, the BER was again brought down to acceptable levels with the application of a RS(255,191) code.

4.3. Bit error rate with FEC — fixed vertical offset

In Fig. 6(d) and Fig. 6(e), BER measurements are recorded at fixed vertical distances and lateral distances ranging between 0 and 50 cm. The fixed vertical distances are set to 2.1 and 2.8 m respectively. In both cases three different Reed–Solomon codes are tested. At a vertical distance of 2.1 m, even the weakest RS(255,247) code is sufficient to achieve error free detection at a lateral distance of 20 cm. However, as the lateral distance is increased to 30 cm, only the strongest RS(255,191) provides a satisfactory BER. This trend continues when the vertical distance is increased to 2.8 m. Regardless of vertical distance and applied FEC code, the BER in each test converges to significantly higher value when the lateral distance is increased to 40 cm. This result is expected, as the raw BER for lateral distances at 40 cm is greater than 10^{-2}.

4.4. Angular dependence

In addition to vertical and lateral motion, rotational motion was also considered. In Fig. 6(f), the effect of rotational motion on BER was recorded for angles ranging from 0° to 45°. In each case BER measurements were recorded as a function of vertical position with a fixed angular rotation. From Fig. 6(f), it is clear that a rotation of 15° can be reasonably tolerated, while angular rotations greater than 15° significantly affect BER performance. This result is consistent with the known viewing angle of the receiving photodiode.

4.5. Bit error rate as a function of data rate

Next we evaluated BER in terms of transmission speed. For this test we sent 10^8 pseudo random bits across the FSO channel without FEC coding and recoded the BER. This test was performed at distances of 1.6, 2.0, and 2.4 m. At each of those distances, results were recorded for data rates ranging from 1 to 50 Mbps. The results of this test are shown in Fig. 7(a). When the data rate is set to 30 Mbps or less, the BER is within acceptable limits for all three distances. As the rate increases further, the BER begins to increase rapidly. Fig. 7(b) summarizes our BER evaluation via a histogram plot containing the maxim possible transmission rates as a function of distance given a BER requirement of 10^{-4} or 10^{-8}. With FEC coding, a BER of 10^{-4} can be converted into a BER of 10^{-8} with very little overhead and is therefore a reasonable target. In its current form, our FSO system is capable of a maximum transmission rate of 50 Mbps,

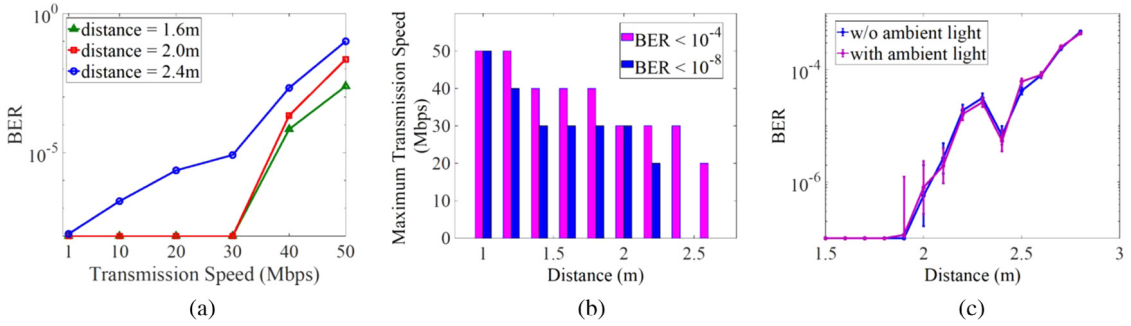

Fig. 7. Data throughput analysis — (a) BER comparison at various data rates, (b) maximum achievable data rates given set BER requirements, (c) ambient light effect on BER.

although range is limited at that rate. At distances approaching 3 m, the maximum throughput for un-coded data with a BER less than 10^{-4} drops to 20 Mbps. The maximum data throughput of this system is in all cases limited by the maximum modulation speed of the transmitting LEDs. In a future version of this project, the LEDs will be replaced with much faster responding laser diodes.

4.6. Ambient light effect

A comparison of system performance with and without ambient light in the room was made to ensure system reliability in ambient lighting conditions. The chance of ambient light interference in our system is low due to the fact that the photodiode that we selected for our receiver comes packaged with an 850 nm optical filter, but the possibility must still be ruled out. Fig. 7(c) show the performance of the FSO system with and without ambient light in terms of BER and vertical distance. It is clear from this plot that the ambient light in the room does not play a significant role in the performance of this system.

When considered together, the evaluations presented in this section make a compelling argument for the viability of our FSO WiFO system in an indoor environment. We have shown that this system is capable of reliably transmitting data at a maximum rate of 50 Mbps and can transmit over distances of up to 3 m. Additionally, we have shown that the BER of this system can significantly be improved through the application of efficient Reed–Solomon FEC codes.

4.7. Evaluation of FSO and WiFi channel throughputs

Now that we have established the capability of the FSO channel as a standalone link, we will consider an experiment that combines both the FSO and WiFi channels together. In this experiment, we will model a scenario in which a WiFi network is artificially congested due to heavy traffic. In this scenario two applications will be running simultaneously. The first application will only have access to the WiFi channel. The second application will use our WiFO protocol and will have access to both the WiFi and FSO channels. The data throughput for both channels will be monitored over time as background traffic is increased and then throttled. This test will last for approximately 300 s with the background traffic being increased after 100 s and then decreased 200 s later. The results of this test are shown in Fig. 8. As expected, the throughput for the WiFi only application is significantly reduced from roughly 8 Mbps to 3.5 Mbps when the background traffic is increased after 100 s. After almost 300 s, the background traffic is throttled back to its original level and the throughput of the WiFi only application increases back up to approximately 8 Mbps. In contrast, the second application does not show any loss of throughput and maintains a 12 Mbps link regardless of background traffic. The FSO channel in the second application provides the bandwidth and flexibility that is necessary for a consistently high-speed link. The fluctuations that are observed in the second application's throughput can be attributed to delays caused when acknowledgments from the receiver are sent back to the AP through the WiFi channel. Data

Table 4
Handoff transition times.

	FSO to WiFi	WiFi to FSO
Light traffic	49.10 ms	1.59 ms
Heavy traffic	87.02 ms	1.64 ms

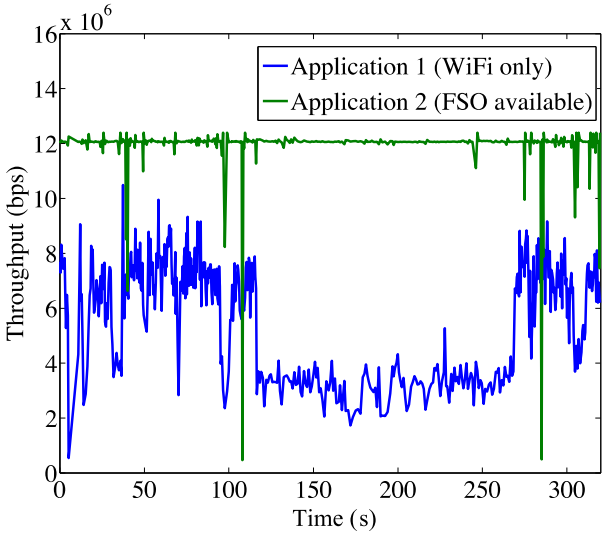

Fig. 8. Throughput comparison between the FSO and WiFi channels.

was also collected on the round trip time for a FSO channel frame, which is the combined time it takes for a frame to be transmitted across the FSO channel and for the AP to receive and acknowledgment of delivery. Fig. 9 shows the round trip time for 80,000 frames containing 600 bytes each. The vast majority of frames were delivered in less than 390 ms, although some statistical outliers do exist.

4.8. Transition time analysis

The final aspect of our WiFO system that we will evaluate is the handoff between the FSO and WiFi channels. A smooth and immediate handoff is essential to ensuring mobility, which is a central aspect of any wireless network. When a receiver first moves into a FSO light cone, the transition time is recorded as the time between the first beacon signal and the first packet received through the FSO channel. When a receiver moves out of a FSO light cone, the transition time is recorded as the time between the receiver timeout and the first packet received through the WiFi channel. Transition times are heavily dependent on network traffic, so transition time data was collected under both heavy and light traffic conditions. The results of those measurements are shown in Table 4. Even under the worst-case scenario, the transition for the FSO channel to the WiFi channel, the transmission time is still less the 100 ms. That

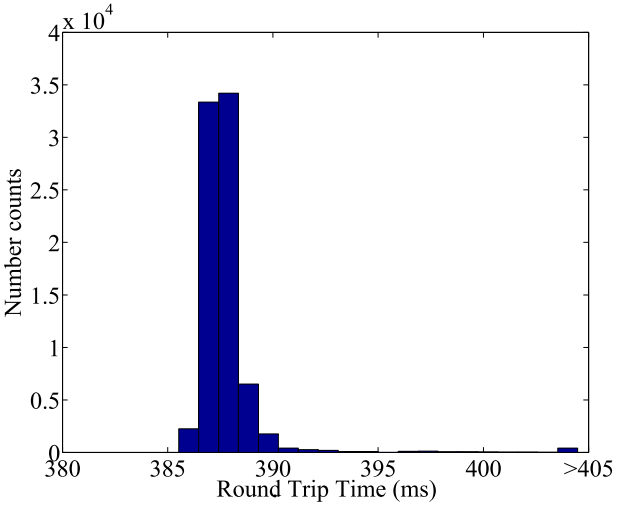

Fig. 9. Rounds trip times in the FSO channel.

amount of time is virtually imperceptible to humans and is therefore acceptable for even latency sensitive applications. The transition time from WiFi to the FSO channel is less than 2 ms regardless of traffic conditions.

5. Conclusion

In this paper, we have presented a novel hybrid FSO and RF wireless communication network architecture, namely, a WiFO system. This architecture improves wireless system performance by utilizing both RF frequencies and spectrum in the optical regime. Through optimized design and integration of the optical transmitters and receivers using off-the-shelf optoelectronic devices, the FSO femtocells in this system deliver up to 50 Mbps over a distance of three meters with a field of view of ±15° and bit error rates between 10^{-6} and 10^{-4}. The bit error rate in this system was further reduced to below 10^{-7} by applying Reed–Solomon FEC codes. Unlike most existing FSO systems using static optical transceivers, we achieved user mobility in this architecture through a unique WiFi-enabled protocol that allows seamless handoff between the optical and WiFi channels. We have experimentally demonstrated the potential of this WiFO architecture by comparing the throughput of our system with a standard WiFi link in a realistic use scenario. Our experimental results have shown that our WiFO architecture is capable of expanding the capacity of existing wireless networks without sacrificing mobility.

Acknowledgment

This work is supported by the National Science Foundation, United States under Grant NSF: EARS 1547450 and the Navy SBIR contract number N6833518C0562.

References

[1] Cisco visual networking index, 2016, Available: http://www.cisco.com/c/en/us/solutions/collateral/service-provider/visual-networking-index-vni/complete-white-paper-c11-481360.html.
[2] FC Spectrum Policy Task Force, Report of the spectrum efficiency working group, Available: http://www.fcc.gov/sptf/reports.html.
[3] Qin Zhao, B.M. Sadler, A survey of dynamic spectrum access, IEEE Signal Process. Mag. 24 (2007) 79–89.
[4] J. Mitola III, G.Q. Maguire Jr., Cognitive radio: making software radios more personal, Pers. Commun. IEEE 6 (4) (1999) 13–18.
[5] A.T. Hussein, J.M.H. Elmirghani, Mobile multi-gigabit visible light communication system in realistic indoor environment, J. Lightwave Technol. 33 (2015) 3293–3307.
[6] I. Stefan, H. Haas, Hybrid visible light and radio frequency communication systems, in: IEEE 80th Vehicular Technology Conference, 2014, pp. 1–5.
[7] S. Bloom, W. Hartley, The Last-Mile Solution: hybrid FSO Radio, AirFiber Inc., 2002.
[8] H. Wu, B. Hamzeh, M. Kavehrad, Achieving carrier class availability of fso link via a complementary rf link, in: Signals, Systems and Computers, 2004. Conference Record of the Thirty-Eighth Asilomar Conference on, vol. 2, 2004, 1483–1487.
[9] A. Abdulhussein, A. Oka, T.T. Nguyen, L. Lampe, Rateless coding for hybrid free-space optical and radio-frequency communication, IEEE Trans. Wirel. Commun. 9 (2010) 907–913.
[10] D. Wang, A. Abouzeid, Throughput capacity of hybrid radio-frequency and free-space-optical (rf/fso) multi-hop networks, in: Information Theory and Applications Workshop, 2007, Jan. 2007, pp. 3–10.
[11] A. Eslami, S. Vangala, H. Pishro-Nik, Hybrid channel codes for efficient fso/rf communication systems, IEEE Trans. Commun. 58 (2010) 2926–2938.
[12] Y. Tang, M. Brandt-Pearce, S. Wilson, Link adaptation for throughput optimization of parallel channels with application to hybrid fso/rf systems, IEEE Trans. Commun. 60 (2012) 2723–2732.
[13] F. Ahdi, S. Subramaniam, Optimal placement of fso links in hybrid wireless optical networks, in: Global Telecommunications Conference (GLOBECOM 2011), IEEE, 2011, pp. 1–6.
[14] N. Letzepis, K. Nguyen, A. Guillen Fabregas, W. Cowley, Outage analysis of the hybrid free-space optical and radio-frequency channel, IEEE J. Sel. Areas Commun. 27 (2009) 1709–1719.
[15] M.Z. Afgani, H. Haas, H. Elgala, D. Knipp, Visible light communication using ofdm, in: 2nd International Conference on Testbeds and Research Infrastructures for the Development of Networks and Communities. TRIDENTCOM, 2006, pp. 6–134.
[16] H. Al Hajjar, B. Fracasso, D. LerouxIndoor, Optical wireless Gbps link dimensioning, in: National Fiber Optic Engineers Conference, Anaheim, CA, 2013, pp. 17–21.
[17] M. Kavehrad, Sustainable energy-efficient wireless applications using light, IEEE Commun. Mag. (2010) 66–73.
[18] K. Wang, A. Nirmalathas, C. Lim, E. Skafidas, Ultra-broadband indoor optical wireless communication system with multimode fiber, Opt. Lett. 37 (2012) 1514–1516.
[19] C. Kottke, J. Hilt, K. Habel, J. Vučić, K.-D. Langer, 1.25 gbit/s visible light wdm link based on dmt modulation of a single rgb led luminary, in: European Conference and Exhibition on Optical Communication, Optical Society of America, 2012, p. We.3.B.4.
[20] G. Cossu, A.M. Khalid, P. Choudhury, R. Corsini, E. Ciaramella, 2.1 gbit/s visible optical wireless transmission, in: European Conference and Exhibition on Optical Communication, Optical Society of America, 2012, p. P4.16.
[21] Y. Wang, Y. Wang, N. Chi, J. Yu, H. Shang, Demonstration of 575- mb/s downlink and 225-mb/s uplink bi-directional scm-wdm visible light communication using rgb led and phosphor-based led, Opt. Express 21 (2013) 1203–1208.
[22] Y. Zheng, M. Zhang, Visible light communications-recent progresses and future outlooks, in: Photonics and Optoelectronic (SOPO) Symposium, 2010, pp. 1–6.
[23] W.O. Popoola, Impact of vlc on light emission quality of white leds, J. Lightwave Technol. 34 (2016) 2526–2532.
[24] H.L. Minh, D. O'Brien, G. Faulkner, L. Zeng, K. Lee, D. Jung, Y. Oh, 80 mbit/s visible light communications using pre-equalized white led, in: Optical Communication 34th European Conference, 2008, pp. 1–2.
[25] L. Grobe, A. Paraskevopoulos, J. Hilt, D. Schulz, F. Lassak, F. Hartlieb, C. Kottke, V. Jungnickel, K.-D. Langer, High speed visible light communication systems, IEEE Commun. Mag. 51 (2013) 60–66.
[26] J. Vucic, C. Kottke, S. Nerreter, K.-D. Langer, J. Walewski, 513 mbit/s visible light communications link based on dmt-modulation of a white led, J. Lightwave Technol. 28 (2010) 3512–3518.
[27] A. Khalid, G. Cossu, R. Corsini, P. Choudhury, E. Ciaramella, 1-gb/s transmission over a phosphorescent white led by using rateadaptive discrete multitone modulation, IEEE Photon. J. 4 (2012) 1465–1473.
[28] Krzysztof Szczerba, Petter Westbergh, Johnny Karout, Johan S. Gustavssin, Asa Haglund, Magnus Karlsson, Peter A. Andrekson, Erik Agrell, Anders Larsson, 4-pam for high-speed short-range optical communications, J. Opt. Commun. Netw. 4 (11) (2012).
[29] Moshe Medina, David Kin, Alex Shar, Yishai Gourman, Ariel Carmeli, Slava Krylov, Micro mirrors for MEMS based free space point to point indoor wireless optical network (IWON), in: IEEE International Conference on Optical MEMS and Nanophotonics, 2015, pp. 2–5.
[30] Huanhuan Zheng, Zhaowen Xu, Changyuan Yu, Mohan Gurusamy, A 3-D high accuracy positioning system based on visible light communication with novel positioning algorithm, Opt. Commun. 396 (2017).
[31] J. McKendry, D. Massoubre, S. Zhang, B. Rae, R. Green, E. Gu, R. Henderson, A. Kelly, M. Dawson, Visible-light communications using a cmos-controlled micro-light- emitting-diode array, J. Lightwave Technol. 30 (2012) 61–67.
[32] A. Burton, E. Bentley, H.L. Minh, Z. Ghassemlooy, N. Aslam, S.-K. Liaw, Experimental demonstration of a 10base-t ethernet visible light communications system using white phosphor light-emitting diodes, Circuits, Dev. Syst. IET 8 (2014) 322–330.
[33] S. Liverman, Q. Wang, Y. Chu, T. Duong, D. Nyuyen-Huu, S. Wang, T. Nguyen, A.X. Wang, Integrating free-space optical communication links with existing wifi (wifo) network, in: SPIE Photonics West, 2015, pp. 97720P–97720P.

[34] H. Elgala, R. Mesleh, H. Haas, Indoor optical wireless communication: potential and state-of-the-art, IEEE Commun. Mag. 49 (2011) 56–62.
[35] Di Wang, Alhussein A. Abouzeid, Throughput and delay analysis for hybrid radio-frequency and free-space-optical (RF/FSO) networks, Wirel. Netw. 17 (2011) 877–892.
[36] O. Bouchet, M. El Tabach, M. Wolf, D. O'brien, G. Faulkner, J.W. Walewski, S. Randel, M. Franke, S. Nerreter, K.-D. Langer, J. Grubor, T. Kamalakis, Hybrid wireless optics (HWO): Building the next-generation home network, in: CNSDSP, 2008, pp. 283–287.
[37] Y. Wang, X. Wu, H. Haas, Distributed load balancing for Internet of Things by using Li Fi and RF hybrid network, in: IEEE 26th Annual International Symposium on Personal, Indoor, and Mobile Radio Communications, 2015, pp. 1289–1294.
[38] H. Haas, L. Yin, Y. Wang, C. Chen, What is lifi? J. Lightwave Technol. 34 (2016) 1533–1544.
[39] Hao Ma, Lutz Lampe, Steve Hranilovic, Hybrid visible light and power line communication for indoor multiuser downlink, J. Opt. Commun. Netw. 9 (8) (2017).
[40] Q. Wang, T. Nguyen, A.X. Wang, Channel capacity optimization for an integrated wi-fi and free-space communication system (wififo), in: Proceedings of the 17th ACM International Conference on Modeling, Analysis and Simulation of Wireless and Mobile Systems, 2014, pp. 327–330.
[41] Qiwei Wang, Spencer Liverman, Yu-jung Chu, Anindita Borah, Songtao Wang, Thinh Nguyen, Arun Natarajan, Alan Wang, WiFO: A Hybrid WiFi free-Space optical communication networks of femtocells, in: MSWiM Conference, 2017, pp. 35-42.
[42] J. Wang, C. Jiang, H. Zhang, X. Zhang, V.C.M. Leung, L. Hanzo, Learning-aided network association for hybrid indoor LiFi-WiFi systems, IEEE Trans. Veh. Technol. 67 (4) (2018) 3561–3574.
[43] X. Wu, M. Safari, H. Haas, Access point selection for hybrid Li-Fi and Wi-Fi networks, IEEE Trans. Commun. 65 (12) (2017) 5375–5385.
[44] H. Alshaer, H. Haas, Bidirectional LiFi attocell access point slicing scheme, in: IEEE Transactions on Network and Service Management.
[45] T. Kishi, H. Tanaka, Y. Umeda, O. Takyu, A high-speed led driver that sweeps out the remaining carriers for visible light communications, J. Lightwave Technol. 32 (2014) 239–249.
[46] Yu-Jung Chu, Mobility Protocol, Channel Estimation and Modulation Techniques for Hybrid Wifi-Fso (Wifo) Wlan of Femtocells (thesis (M.S.)), Degree Granting Institute, Oregon State University, 2016.